Photoluminescence Characteristics of Multilayer Al/ZnO/SiO_2 Structures Grown on Silicon Substrates by DC Reactive Magnetron Sputtering Technique

Oday A. Hammadi

Department of Physics, College of Education, Al-Iraqia University, Baghdad, IRAQ
Email: oday.hammadi@aliraqia.edu.iq

Abstract
In this work, multilayer structures were fabricated on silicon substrates by dc reactive magnetron sputtering technique. Different layers from silicon dioxide (SiO_2), zinc oxide (ZnO), and aluminum (Al) were deposited with different thicknesses to compare different multilayer structures by recording their photoluminescence (PL) spectra in the spectral range of 200-1100 nm. The structure of Al/ZnO/SiO_2/Si showed higher PL intensity than those of other structures due to the radiative activity of ZnO in addition to the important role of aluminum layer to enhance the PL signal as a result of the localized surface plasmon resonance (LSPR) at the interface between Al and ZnO layers.

Keywords: Photoluminescence; Silicon-based structures; Multilayer structures; Zinc oxide
Received: December 2025; **Revised:** February 2026; **Accepted:** February 2026; **Published:** April 2026

1. Introduction

The transparent conducting oxides (TCOs) represent the cornerstone to develop the next generation of optoelectronic devices such as solar cells, light-emitting diodes (LEDs), and flat displays. Zinc oxide (ZnO) – as a TCO – is considered as an ideal candidate due to its wide direct energy band gap (~3.37eV) at room temperature, high excitonic binding energy (60 meV), which guarantees high photoluminescence efficiency at elevated temperatures [1-6]. Despite the featured characteristics of pure ZnO, the enhancement of its performance requires the incorporation of other elements or forming multilayer structures. Doping ZnO with aluminum (Al) or adding aluminum as a thin layers within the multilayer structure – known as AZO – very active way to increase the charge carrier concentration and enhance the electrical conductivity with no effect on the optical transparency in the visible region of electromagnetic spectrum [7-9]. When aluminum atoms are incorporated as donor dopants in the ZnO lattice structure, a noticeable change in the optical characteristics may result due to the increase in the concentration of free carriers according to the Burstein-Moss effect as the optical energy band gap increases due to filling the lower states in the conduction band with excess electrons. The understanding of this effect is necessary to interpret the changes in optical transmission and absorption characteristics of the multilayer structures at different doping levels [10-12].

To explain the practical advantages of the multilayer Al/ZnO/SiO_2/Si structures, the individual roles of each layer is indicated. Since silicon shows weak light emission due to indirect band gap, then the incorporation of an optically active layer, such as ZnO, may facilitate the production of light-emitting diodes (LEDs) in integrated circuits (ICs) at lower cost and reduced size for optical communication systems [25-27]. Also, such multilayer structures can be used as windows or front electrodes in solar cells to increase the energy conversion efficiency [28,29]. Such multilayer structures can be employed in the fabrication of thin-film transistors (TFTs) for touch screens and transparent displays. They provide an ideal balance between high transmittance and low electrical resistance for flexible and transparent displays as the control of photoluminescence characteristics ensures the purity of display colors [30-32].

The aim of this work is to introduce the synergetic effects of the multilayer Al/ZnO/SiO_2 structures grown on silicon substrates by studying the photoluminescence characteristics and their dependencies on crystalline structure and surface topography.

2. Experimental Part

A dc reactive magnetron sputtering system was used in this work to prepare the multilayer structures on silicon substrates. The cleaning of silicon substrates is considered as the fundamental and

crucial step in fabrication of semiconducting structures for optoelectronics because even the slight surface contamination can result in defects within the deposited layers, which directly affect the electrical and optical properties of the final device. Cleaning step is started by removing the organic residuals such as oils, sticking materials and fingerprints. For this purpose, organic solvents are used consequently as the substrates are immersed in acetone for 5 minutes inside an ultrasonic bath to break the stuck organic layers, then directly transferred to ethanol to remove the residual acetone and prevent the formation of any organic thin layers due to its evaporation. Then the substrates are rinsed thoroughly in de-ionized (DI) water to remove the traces of the solvents.

After cleaning with organic materials, a standard cleaning method – known as RCA cleaning – containing two steps is applied. In the first step, the substrates are immersed for 15 minutes in a solution of de-ionized water, ammonium hydroxide (NH_4OH), and hydrogen peroxide (H_2O_2), with mixing ratio of 5:1:1, respectively, to remove residual micro-particles and contaminants. This solution can oxidize and dissociate the organic impurities in addition to separate the micro-particles from the substrate surface. The substrates are then rinsed in DI water to remove the residual solution. In the second step, the metallic contaminants are removed by immersing the silicon substrates in a solution containing DI water, hydrochloric (HCl) acid, and H_2O_2 with mixing ratio of 6:1:1, respectively, for 10 minutes at 70-80 °C. This solution dissolves the metallic ions existed on the substrate surface or trapped with the surface oxide layer. Then, the substrates are rinsed thoroughly in DI water to remove the residual acid.

In most optoelectronics applications, the naturally-formed oxide layers on the silicon surface are not desired, therefore, the steps mentioned above are followed by immersion of the cleaned substrates in a diluted solution (1-2%) of hydrofluoric (HF) acid for few seconds to remove the SiO_2 layer might be grown on the surface and forming an H-terminated surface, which shows lower chemical activity for short time, then rinsed in DI water, carefully dried using dry nitrogen gas.

After completing the cleaning procedure, the silicon substrates are transferred to plasma chamber and subjected to plasma discharge for 10 minutes to activate the surface before deposition process is started because exposure to plasma leads to break the residual organic bonds and hence increase the surface energy. This would enhance the homogeneity and adhesion of the thin layers to be deposited later.

The preparation of the multilayer structures is started with the deposition of 200 nm SiO_2 layer by sputtering a silicon target in existence of oxygen gas in the gas mixture ($Ar:O_2$) with mixing ratio of 10:90 for 120 minutes. The sample is left to cool down to the room temperature before changing the sputtering target by zinc (Zn) to repeat the sputtering process using $Ar:O_2$ gas mixture with mixing ratio of 50:50 to deposit a 150 nm layer of ZnO after 90 minutes. The sample is left to cool down to the room temperature and the sputtering target is replaced by aluminum (Al) sheet to deposit a 100 nm layer of aluminum over the ZnO layer after 45 minutes. The sample is left inside the deposition chamber under vacuum for 24 hours to ensure the chemical and structural stabilities. Then, the samples are transferred to the characterization systems to carry out the absorption and photoluminescence measurements. A Spectra Academy KMAC S2100 spectrophotometer was used to record these spectra in the spectral range of 200-1100 nm. Figure (1) shows schematically the steps to prepare multilayer structure in this work.

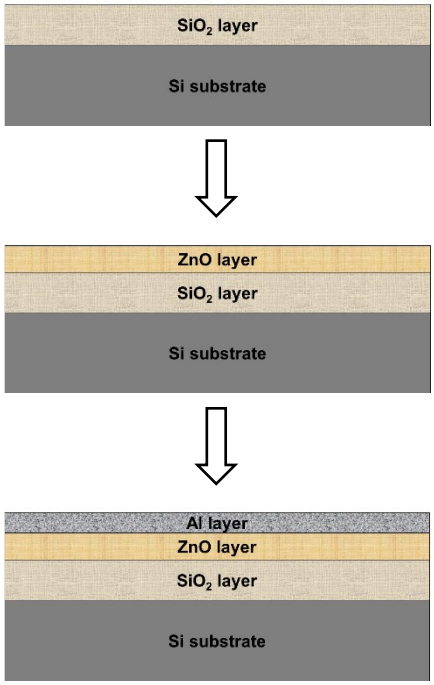

Fig. (1) Schematic diagram of the experimental steps to prepare the multilayer structures of Al/ZnO/SiO_2/Si in this work

3. Results and Discussion

Figure (2) shows the photoluminescence (PL) spectra of the prepared multilayer structures using a UV laser of 385 nm as an excitation source, whose spectrum is seen as a sharp peak on the left. This wavelength was selected according to the absorption spectra of the prepared samples because laser source can provide reasonably high intensity with monochromaticity to ensure high response of the samples. All samples show emission spectra within the range 500-560 nm (visible region) with peaks centered around 530-540 nm. Such emission is usually attributed to the emissions from oxygen vacancies of interband states in metal oxide (SiO_2 and

ZnO) molecules, which refers to the same fundamental mechanism of fluorescence in all samples regardless the existence or absence of the ZnO and Al layers. Also, the sequence of the deposited layers was found to affect the intensity of the spectrum but not the emission peak. These spectra are reasonably wide due to the multiple radiative centers in the ZnO layer, defect distribution, and the effects of inter-reaction between the different layers.

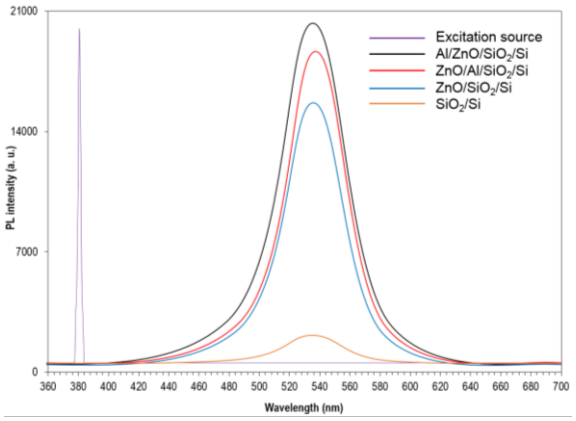

Fig. (2) PL spectra of the multilayer structures prepared in this work

The Al/ZnO/SiO_2/Si structure shows the maximum PL intensity while the SiO_2/Si structure shows the minimum intensity. This difference is ascribed to the important role of aluminum layer to enhance the PL signal as a result of the localized surface plasmon resonance (LSPR) at the interface between Al and ZnO layers. The existence of aluminum leads to increase the local electromagnetic field near the ZnO layer, which increase the probability to absorb the excitation photons and hence increase the rate of radiative transitions and consequently the PL intensity. As well, the existence of the dielectric SiO_2 layer between the Si substrate and ZnO layer reduces the non-radiative recombination, limits the energy loss as heat, and increase the photo-emission efficiency. The ZnO/SiO_2/Si structure shows lower intensity than the Al/ZnO/SiO_2/Si structure due to the absence of the plasmonic amplification effects attributed to the aluminum layer. The SiO_2/Si structure actually exhibits very poor PL as it lacks to a photo-active material such as ZnO, therefore, its signal may be a noise or emission activity due to the defects or secondary oxide phases present at the interface between SiO_2 and Si surface.

The differences in the peak position or spectrum width are resulted from the differences in the microstructures, lattice stresses, and the nature of interfaces between layers. For example, in case of the ZnO/Al/SiO_2/Si structure, the existence of Al layer may reasonably affect the surface morphology of the next ZnO layer during deposition or heat treatment, which leads to modify the density of surface defects of re-distribute the inter-band states within the energy bandgap. As well, the difference between the spectra of the Al/ZnO/SiO_2/Si and ZnO/Al/SiO_2/Si structures may change the conditions of reflection and optical interference within each structure, which may enhance or reduce specific parts of the PL spectrum due to the constructive and destructive interferences. Therefore, these spectra are attributed to ZnO radiative activity in addition to the optical, plasmonic, and inter-band effects within the whole multilayer structures.

4. Conclusion

In concluding remarks, different layers from silicon dioxide (SiO_2), zinc oxide (ZnO), and aluminum (Al) were deposited with different thicknesses to compare different multilayer structures by recording their photoluminescence (PL) spectra in the spectral range of 200-1100 nm. The structure of Al/ZnO/SiO_2/Si showed higher PL intensity than those of other structures due to the radiative activity of ZnO in addition to the important role of aluminum layer to enhance the PL signal as a result of the localized surface plasmon resonance (LSPR) at the interface between Al and ZnO layers.

References

[1] J.M. Shainline, “Optoelectronic intelligence”, *Appl. Phys. Lett.*, 118 (2021) 160501.

[2] J. Cheng et al., “Recent Advances in Optoelectronic Devices Based on 2D Materials and Their Heterostructures”, *Adv. Opt. Mater.*, 7(1) (2019) 1800441.

[3] O.A. Hammadi, M.K. Khalaf, F.J. Kadhim, “Fabrication of UV Photodetector from Nickel Oxide Nanoparticles Deposited on Silicon Substrate by Closed-Field Unbalanced Dual Magnetron Sputtering Techniques”, Opt. Quantum Electron., 47(12) (2015) 3805-3813.

[4] D. Ziental et al., “Titanium Dioxide Nanoparticles: Prospects and Applications in Medicine”, *Nanomater.*, 10 (2020) 387-31.

[5] F.I. Ezema A.B.C Ekwealor and R.U. Osuji, “Optical properties of chemical bath deposited nickel oxide (NiO_x) thin films”, *Superficies y Vacío*, 21(1) (2008) 6-10.

[6] H. Sadiq et al., “Preparation and photocatalytic degradation of ZnO/Fe_3O_4/GO heterojunction via synergistic electron-hole separation”, *Mater. Sci. Eng. B*, 324(A) (2026) 118903.

[7] O.A. Hammadi et al., “Operation Characteristics of a Closed-Field Unbalanced Dual-Magnetrons Plasma Sputtering System”, Bulg. J. Phys., 41(1) (2014) 24-33.

[8] G. Li et al., “Enhanced chemiresistive sensing performance of well-defined porous CuO-doped ZnO nanobelts toward VOCs”, *Nanoscale Adv.*, 1(10) (2019) 3900-3908.

[9] K.A. Jagadish and D. Kekuda, “Performance analysis of a DC magnetron sputtered Cu_2O/TiO_2

heterojunction photodetector for short-wavelength detection", *Sens. Actuat. A: Phys.*, 388 (2025) 116517.
[10] O.A. Hamadi, "Profiling of Antimony Diffusivity in Silicon Substrates using Laser-Induced Diffusion Technique", *Iraqi J. Appl. Phys. Lett.*, 3(1) (2010) 23-26.
[11] J.A. Yaseen, "Effects of Silicon Dioxide Layer on Optoelectronic Characteristics of FeO/PSi Heterostructures", *Iraqi J. Appl. Phys. Lett.*, 8(4) (2025) 99-102.
[12] J.W. Yang et al., "Nanoporous oxide electrodes for energy conversion and storage devices", *RSC Appl. Interfaces*, 1(1) (2024) 11-42.
[13] L. Wang et al., "Progress and perspectives of self-powered gas sensors", *Next Mater.*, 2 (2024) 100092.
[14] R.H. Turki and M.A. Hameed, "Spectral and Electrical Characteristics of Nanostructured NiO/TiO_2 Heterojunction Fabricated by DC Reactive Magnetron Sputtering", *Iraqi J. Mater.*, 3(3) (2024) 39-44.
[15] M. Coll et al., "Towards Oxide Electronics: a Roadmap", *Appl. Surf. Sci.*, 482 (2019) 1-93.
[16] M. Lu et al., "Cu_2O/Co_3O_4 nanoarrays for rapid quantitative analysis of hydrogen sulfide in blood", *Nanoscale Adv.,* 5(6) (2023) 1784-1794.
[17] M.M. Ahmed and R.S. Behnam, "Sheet Resistance of Cobalt/Silicon Ohmic Contacts Fabricated by Laser-Induced Diffusion", *Iraqi J. Appl. Phys. Lett.*, 7(4) (2024) 3-5.
[18] J.A. Yaseen, "Influence of FeO Layer Thickness on Characteristics of FeO/Porous Silicon Heterojunction Photodetectors", *Iraqi J. Mater.*, 4(4) (2025) 153-162.
[19] M.-Y. Dai et al., "First-principles calculations of the photocatalytic performance of ZnO–MX_2 (M = Mo, W; X = S, Se) heterojunctions", *RSC Adv.*, 15(29) (2025) 23489-23498.
[20] N. Alomayrah et al., "Fabrication of a highly efficient CuO/$ZnCo_2O_4$/CNTs ternary composite for photocatalytic degradation of hazardous pollutants", *RSC Adv.*, 14(34) (2024) 24874-24897.
[21] N.A.H. Hashim and T.A. Almashhadani, "Optoelectronic Characteristics of Co_3O_4 NPs/PSi/Si Photodetector", *Iraqi J. Appl. Phys. Lett.*, 9(1) (2026) 34-37.
[22] N.A.H. Hashim, F.J. Kadhim and Z.S. Abdulsattar, "Characterization of Electrochromism and Photoelectrochromism of N-Doped TiO_2 and Co_3O_4 Thin Films Prepared by DC Reactive Magnetron Sputtering: Comparative Study", *Iraqi J. Appl. Phys.*, 19(1) (2023) 5-12.
[23] N.M. Hieu et al., "ZnTe-coated ZnO nanorods: Hydrogen sulfide nano-sensor purely controlled by pn junction", *Mater. Design*, 191 (2020) 108628.
[24] Q.F. Sadoon, M.S. Jassem and A.J. Nasori, "Morphological Characteristics of Plasma-Etched Silicon Substrates Coated with Nickel Oxide Nanoparticles for Optoelectronics Applications", *Iraqi J. Appl. Phys. Lett.*, 7(4) (2024) 6-8.
[25] R.K. Paul and Md. Ahmaruzzaman, "Advanced photocatalytic degradation of POPs and other contaminants: a comprehensive review on nanocomposites and heterojunctions", *RSC Adv.*, 15(38) (2025) 31313-31359.
[26] R.N. Khoshnaw, "Characteristics of CoO/Si Heterostructure Prepared by Plasma-Induced Bonding", *Iraqi J. Appl. Phys. Lett.*, 7(2) (2024) 19-22.
[27] S. Tahiri, "Heterojunction Solar Cell Based on Highly-Pure Nanopowders Prepared by DC Reactive Sputtering Technique", *Iraqi J. Mater.*, 3(2) (2024) 77-82.
[28] S.K. Srivastava, "Recent advances in removal of pharmaceutical pollutants in wastewater using metal oxides and carbonaceous materials as photocatalysts: a review", *RSC Appl. Interface.*, 1(3) (2024) 340-429.
[29] V. Paolucci et al., "SnO_2 quantum dot decoration of CuO nanoparticles with enhanced NO_2 and H_2 gas sensing response via p–n heterojunction interfaces", *RSC Adv.*, 15(46) (2025) 38750-38761.
[30] V.S. Ghodake et al., "Exploring the antibacterial properties of ZnO nanorods–CuO nanoflowers: a mode of action approach", *RSC Adv.*, 15(40) (2025) 32995-33005.
[31] N.A.H. Hashim and F.J. Kadhim, "Structural and Optical Characteristics of Co_3O_4 Nanostructures Prepared by DC Reactive Magnetron Sputtering", *Iraqi J. Appl. Phys.*, 18(4) (2022) 31-36.
[32] A.S. Falah and K.R. Jasim, "Simulation Study on Current Gain Improvement at High Collector Current Densities for CuO/TiO_2 Heterostructure Transistors", *Iraqi J. Mater.*, 3(4) (2024) 25-30.

